RAD Conference Proceedings, vol. 7, pp. 52-58, 2023
ISSN 2466-4626 (online) | DOI: 10.21175/RadProc.2023.10
www.rad-proceedings.org

SOME RESULTS FOR THE STUDY OF THE EFFICIENCY AND CROSS-TALK PROBABILITY BY USING GEANT4 SIMULATIONS FOR THE NEUTRON CORRELATOR NARCOS

G. Santagati[1*], E. V. Pagano[2], C. Boiano[3], G. Cardella[1], A. Castoldi[4,3], E. De Filippo[1], E. Geraci[5,1], B. Gnoffo[5,1], C. Guazzoni[4,3], A. Lanzalone[6,2], C. Maiolino[2], N. S. Martorana[1], A. Pagano[1], S. Pirrone[1], G. Politi[5,1], F. Risitano[7,1], F. Rizzo[5,2,8], P. Russotto[2], M. Trimarchi[7,1], C. Zagami[5,2,8].

[1]INFN, Sezione di Catania, via Santa Sofia 62, Catania, 95123, Italy,
[2]INFN, Laboratori Nazionali del Sud, via Santa Sofia 64, Catania, 95123, Italy,
[3]INFN, Sezione di Milano, via Celoria 16, Milano, 20133, Italy,
[4]Politecnico di Milano, Dip. Elettronica, Informazione e Bioingegneria, via Ponzio 34/5, Milano, 20133, Italy,
[5]Università di Catania, Dipartimento di Fisica e Astronomia, via Santa Sofia 64, Catania, 95123, Italy,
[6]Università di Enna "Kore", piazza dell'Università, Enna, 94100, Italy,
[7]Università di Messina, Dipartimento di Scienze MIFT, viale Ferdinando Stagno d'Alcontres 31, Messina, 98166, Italy,
[8]CSFNSM-Centro Siciliano di Fisica Nucleare e Struttura della Materia, via Santa Sofia 64, Catania, 95123, Italy.

Abstract. *Neutron and light-charged particle detections with high angular and energy resolution become mandatory for future experiments with radioactive beams that will be provided by new heavy ion facilities such as FRAISE at LNS, SPES at LNL, and FAIR at GSI. The aim of the ANCHISE project is to use a new-generation plastic scintillator, called EJ276-G, coupled with a SiPM photosensor as the elementary detection cell of a segmented multi-detector able to detect at the same time neutrons and light-charged particles. In this contribution new results, obtained through Monte Carlo simulations, will be described on detection efficiency and cross-talk probability estimation as a function of the incident neutron energy and the detection threshold. Two geometrical configurations of the elementary cells were investigated. The study supports the construction of NArCoS, a neutron correlator based on the EJ276-G scintillator as a basic element coupled with SiPM photosensors, for application in nuclear and applied physics.*

Keywords: *Monte Carlo simulations, Neutrons detector, Plastic scintillator*

1. INTRODUCTION

Heavy ion collisions at Fermi energy are extensively explored in both nuclear reaction and nuclear structure studies. The measurement of particle-particle relative energy correlation is a crucial method to access the dynamics in the early stages of the collision (20–100 fm/c), which has been adopted since the beginning of heavy ion physics to distinguish between prompt (<100 fm/c) and sequential reactions (<1000 fm/c) [1-6]. The light charged particle (LCP) correlations and the correlations of heavier particles as the Intermediate Mass Fragments (IMF), whose typical atomic number are in the range $2 < Z < 25$, have been widely studied in many works, both from the experimental and theoretical sides [5, 7, 8]. On the contrary, only a few investigations have been reported at including uncharged particles in the main trigger, in particular for n-n, n-p, and n-IMF correlations [8, 9, 10]. In order to extract sufficiently accurate experimental information, a good resolution of the relative linear momentum (both in intensity and in the detection angle) represents a key aspect to consider in the study of particle-particle correlations [11, 12, 13].

Recent papers show the accuracy of the plastic scintillator EJ-276, produced by Eljen Technologies [14], as light response function of Birks semi empirical approach [15] over a wide range of charged nuclear particles with energies ranging from 2 to 20 AMeV, in terms of the discriminating power using pulse shape analysis with radioactive sources [16], and in reactions induced by heavy ions [17]. In terms of timing response, a new generation of compact Silicon Photomultiplier (SiPM) arrays directly coupled to the scintillator can provide sub-nanosecond timing resolution [18]. The NArCoS project [11,12,13] (Neutron Array for Correlation Studies) aims at developing a new detector devoted to detect neutrons and light charged particles with high angular and energy resolutions. Conceptually, the prototype configuration is an array of 64 elementary cells of the EJ276-G plastic scintillator. Each elementary plastic (cell) has the dimension of 3x3x3 cm^3 arranged in a cubic geometry and individually read by a SiPM matrix. Assuming a distance of 150 cm from the interaction target, the neutron angular resolution is estimated to be about 1° in the laboratory frame. The kinetic energy neutron measurement is entrusted to the time-of-flight (ToF) technique, for which about 5% of energy resolution is estimated (considering the distance of 150 cm and a 500 ps time resolution). The hodoscope will detect neutrons in nuclear reactions, from light to heavy ion collisions, in the energy range between 10 AMeV ≤ E/A ≤ 100 AMeV. The neutrons in the plastic scintillator are prevalently (at these energies) seen as protons, for this reason, a DSSSD will be used as a veto detector in order to disentangle a primary proton from a

* E-mail of the corresponding author – gianluca.santagati@ct.infn.it

primary neutron. The project will allow to design a second-generation neutron detector (but also light charged particles), aimed at working in a stand-alone mode or coupled to high-granularity 4π-detector systems like CHIMERA [2, 19] or other light charged particle correlators like FARCOS [20-25] at National Laboratories of Sud in Catania (LNS). The neutron correlator is suitable for the incoming facilities for radioactive ion beams (RIBs) like, for example, FRAISE at INFN-LNS [26, 27, 28], SPES at National Laboratories of Legnaro (LNL) [29] and FAIR at GSI Darmstadt [30]. In particular, at GSI, the assembly of NeuLAND [31], a large area neutron detector, designed for the physics program proposed for the R^{3}B facility, will be completed soon. Thanks to the large isospin asymmetry of envisaged ions, it will be possible to deepen the study of in-medium nuclear interaction, the equation of state of nuclear matter, the reaction mechanism as a function of the isospin, and the asymmetric nuclear structure properties of unbound and exotic nuclear states, just to quote a few examples. The project will provide new studies for the three years 2022–2024, focusing on a dedicated readout digital electronic and an optimal mechanical configuration. In the next years, the project will focus on two very important tasks: the evaluation of the detection efficiency and the study of the cross-talk performed both with simulations and with experiments and tests. In this paper, new results, obtained through GEANT4 Monte Carlo simulations [32, 33], will be described about the detection efficiency and the cross-talk probability estimation as function of the incident neutron energy and the elementary cell detection threshold. Two geometrical configurations of the elementary detection cell were investigated.

2. The cross-talk problem

As already mentioned, the elementary cell detection is a cube of 3x3x3 cm^3 of EJ276-G fast plastic scintillator coupled with a SiPM matrix housed on a PCB board. The SiPM matrix dimensions are 30.7 x 30.7 x 0.96 mm^3 while the PCB board dimensions are 40.8 x 40.8 x 1.6 mm^3. The circuit of the prototypal read-out system performs the sum of all the signals of a SiPM matrix in order to have a fast signal, with low noise and amplitude that matches with the energy range of interest and the dynamic range used in the DAQ acquisition. The PCB board has also input/output connectors for the SiPMs power supply, signal output, pulser test input and temperature control. This solution achieves a very compact design that will allow to bring the elementary cells of the detector array as closer as possible. The read-out system is described in detail in Ref. [34].

The elementary detection cell simulated in GEANT4 for all the calculations discussed in this paper is shown in Figure 1.

The basic module is a set of adjacent elementary cells assembled to form a cluster. The final array is obtained by assembling the clusters. It is highly segmented in all directions, including the flight one; the total thickness is enough to ensure a reasonable interaction probability, while segmentation in small size cells a precise position measurement, fundamental for the determination of the time of flight and detec tion angle. The cross-talk effects, coming from neutr-

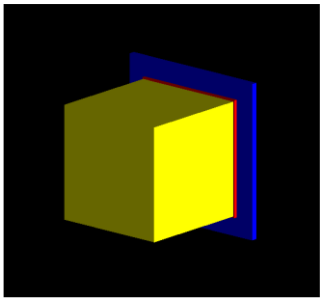

Figure 1. Simulation of the EJ276-G plastic scintillator cell (yellow) with the SiPM matrix (red) and a PCB board (blue).

interacting in two or more detection cells and from re-scatterings of neutrons and gammas in the environmental structure and wall, are a crucial (and typical) problem in experiments aiming at detecting neutrons [9] in a broad range of kinetic energies (from low energy to several tens of MeV). These phenomena simulate unreal reaction events with the neutron multiplicity distorted by the detection of spurious neutron signals (background) inside the active volume of the detector at the same time (defined by a proper time window) as a typical true neutron signal. The segmented geometry helps in studying this effect, as each fired cell produces an independent logical signal, and a pattern is available in order to reconstruct the tracks of the observed single event. Individual timing signals can be exploited to measure the time of flight and the time pattern, which can be used to disentangle true and spurious coincidences.

A preliminary study [13] of the cross-talk was performed by simulating the configuration of a cluster of four elementary scintillator cells in close assembly (parallelepiped) by means of the GEANT4 simulation software. Neutrons from 5 MeV to 50 MeV (5 MeV steps) were considered by assuming exponential forward-peaked angular distributions. The cross-talk probability was estimated by the integration of all the possible event configurations simulated by the software considering a detection threshold of 1.5 MeV. This probability increases slowly from about 1% for 5 MeV up to 9% for 50 MeV of neutrons [13]. Moreover, simulations produce precise evaluations of detector efficiencies as a function of neutron energy.

In this paper, the results of more complete simulations for lower-energy neutrons and lower elementary cell detection thresholds with increasing numbers of cells and different geometric configurations are presented.

3. Simulation description

All the calculations were performed using the Monte Carlo GEANT4 code and the QGSP_BIC_HP libraries. Monochromatic neutrons in air configuration from 1 MeV to 6 MeV (1 MeV steps) and 10 MeV were simulated by assuming forward-peaked angular distributions. The incident neutron flux originates from a plane source placed 150 cm from the configuration considered, according to the NArCoS geometry. The incident neutron flux and its interaction in various materials were well reproduced, and the total energy deposition of neutrons in several materials

was calculated. The detection considered signals with no-threshold and with thresholds of 0.5, 1.0 and 1.5 MeV and the cross-talk probability were given by the integration of all the possible event configurations simulated by the software.

Two different geometrical configurations of the elementary cell were investigated:

1) matrix configuration: it consists of 3x3 elementary cells, as shown in Figure 2;
2) three-cluster configuration: it consists of three adjacent clusters, as shown in Figure 3.

In the first calculations of this study, simulations with and without the SiPM matrix and PBC board were performed in order to estimate its contributions to the overall cross-talk probability. From these calculations, it is possible to affirm that the SiPM matrix and PCB board contributions to the overall cross-talk are basically negligible for the two simulated configurations.

3.1. Cross-talk probability simulation in the matrix configuration

In this geometrical configuration a simulated flux of 10^5 neutrons is impinging on the central cell, as shown in Figure 4.

The study of this geometrical configuration allows to evaluate the distributions of the scattered particles along with the x and y directions.

The cross-talk probability CT is defined by Equation 1:

$$CT = 1 - \frac{\sum_{i=1}^{9} Cell_i}{DET} \quad (1)$$

where DET is the integral of the number of particles detected by the whole matrix detector configuration

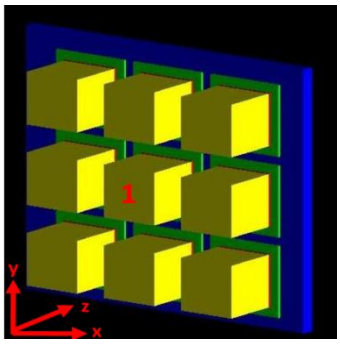

Figure 2. Simulation of the matrix configuration. Central cell (ID=1) and a reference system are also indicated.

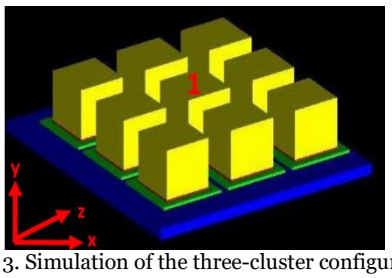

Figure 3. Simulation of the three-cluster configuration. Central cell (ID =1) and a reference system are also indicated.

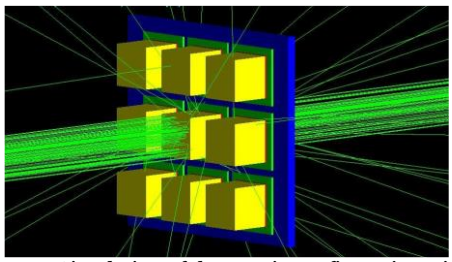

Figure 4. Simulation of the matrix configuration with a neutron flux (green tracks) impinging on the central cell. It is possible to see the scattered and not scattered particles.

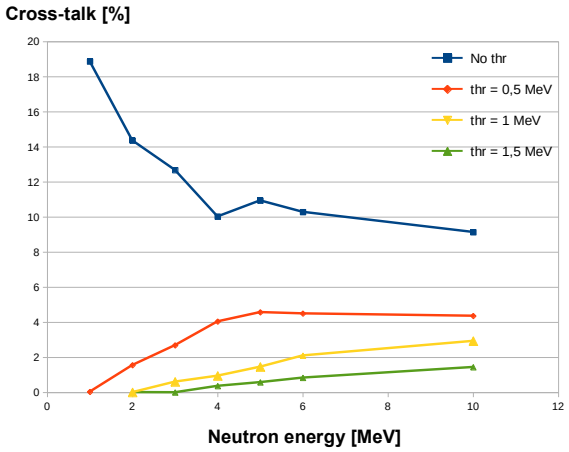

Figure 5. Overall cross-talk percentage values as a function of the neutron flux energy for the matrix configuration. A different curve is plotted for each detection threshold setting in the elementary cell.

and Celli represents the number of particles detected by the one and only cell i (i = 1,...,9). It is easy to understand that the cross-talk probability contributions come from particles that deposited a quantity of energy over the detection threshold at least on two different elementary detection cells.

In Table 1 the overall cross-talk percentage values obtained for the matrix configuration are shown.

Table 1. Overall cross-talk percentage values for different neutron flux energy and different elementary cell detection thresholds obtained in the matrix configuration.

Neutron Energy [MeV]	CT [%] values for different thresholds [MeV]			
	0.0	0.5	1.0	1.5
1	18.87	<0.1	-	-
2	14.36	1.55	<0.1	<0.1
3	12.68	2.68	0.61	<0.1
4	10.02	4.04	0.94	0.37
5	10.94	4.57	1.46	0.58
6	10.29	4.50	2.10	0.83
10	9.14	4.26	2.93	1.44

The overall cross-talk percentage values as a function of the neutron flux energy for the matrix configuration are shown in Figure 5.

Higher cross-talk probabilities are observed for lower detection thresholds, especially for lower energy neutrons, as expected. Values of the cross-talk probability less than 3 % and 2 % are found with detection thresholds of 1 and 1.5 MeV respectively,

even for 10 MeV neutrons that represents the worst case scenario.

3.2. Cross-talk probability simulation in the three-cluster configuration

In this configuration a simulated flux of 10^5 neutrons is impinging on the first cell of the central cluster, as shown in Figure 6.

The study of this geometrical configuration allows to evaluate basically the distributions of the scattered particles along with the z direction (neutron flux direction that simulates the neutron flight direction, (see Introduction).

Considering that the number of cells in this configuration is the same of the previous one, it is still possible to use the cross-talk probability CT defined by the Equation 1, where, now, DET is the integral of the number of particles detected by the whole three-cluster configuration and $Cell_i$ represents the number of particles detected by the one and only cell i (i = 1,...,9).

The overall cross-talk percentage values obtained for the three-cluster configuration are shown in Table 2 and plotted in Figure 7.

Table 2 Overall cross-talk percentage values for different neutron flux energy and different elementary cell detection thresholds obtained in the three-cluster configuration.

Neutron Energy [MeV]	CT [%] values for different thresholds [MeV]			
	0.0	0.5	1.0	1.5
1	19.04	<0.1	-	-
2	16.47	3.91	<0.1	<0.1
3	15.25	5.18	1.63	<0.1
4	14.60	6.20	3.30	0.96
5	13.70	6.38	3.65	1.79
6	13.20	6.23	3.77	2.45
10	11.67	5.61	3.86	2.73

Slightly higher cross-talk probabilities are observed in this configuration with respect to the matrix one, as expected. Even in this case, reasonable values of the cross-talk probability are found with detection thresholds of 1 and 1.5 MeV for 10 MeV neutrons.

4. Efficiency simulation

In order to estimate the efficiency values, monochromatic fluxes of 10^6 neutrons in air configuration from 1 MeV to 6 MeV (1 MeV steps) and

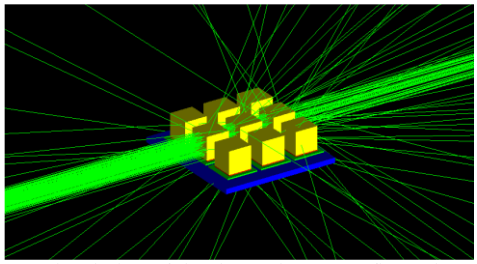

Figure 6. Simulation of the three-cluster configuration with a neutron flux (green tracks) impinging on the first cell of the central cluster. The scattered and not scattered particles are shown.

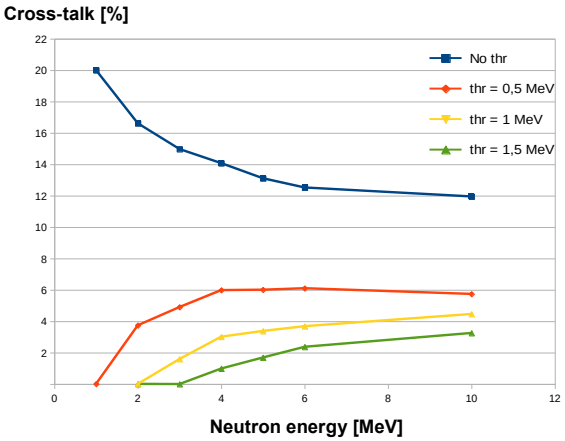

Figure 7. Overall cross-talk percentage values as a function of the neutron flux energy for the three-cluster configuration. The different curves are obtained for different elementary cell detection thresholds.

10 MeV were simulated. The incident neutron flux is geometry), and its dimensions are equal to the surface originated by plane sources placed 150 cm far the detector configuration (according to the NArCoS dimensions of the geometrical configuration considered. The flux was impinging over the entire considered configuration surface with forward-peaked angular distributions, as shown in Figure 8.

The efficiency EFF is defined by the Equation 2:

$$EFF = \frac{TOT}{SIM} \qquad (2)$$

where TOT is the number of particles detected by the whole considered configuration and SIM is the number of neutrons simulated impinging over the entire geometrical configuration surface (10^6). The number of

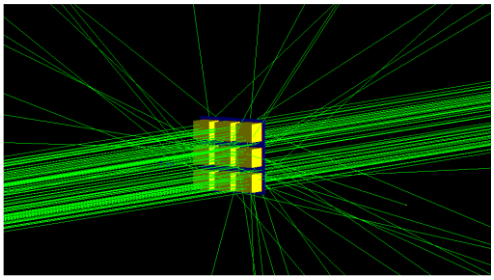

Figure 8. Simulations of the neutron flux impinging over the entire matrix configuration surface.

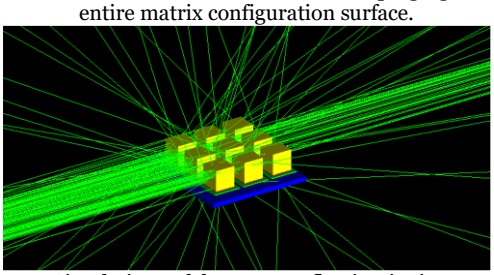

Figure 9. Simulations of the neutron flux impinging over the entire three-cluster configuration surface.

Table 3. Corrected efficiency percentage values evaluated for the matrix configuration for different neutron flux energy and different elementary cell detection thresholds.

Neutron Energy [MeV]	Efficiency [%] values corrected by CT for different thresholds [MeV]			
	0.0	0.5	1.0	1.5
1	52.66	23.14	-	-
2	31.92	23.64	16.26	9.83
3	26.78	22.52	16.42	12.88
4	30.23	24.62	19.14	13.87
5	23.36	19.05	15.82	12.76
6	21.61	18.10	15.62	12.35
10	18.89	14.40	11.59	10.45

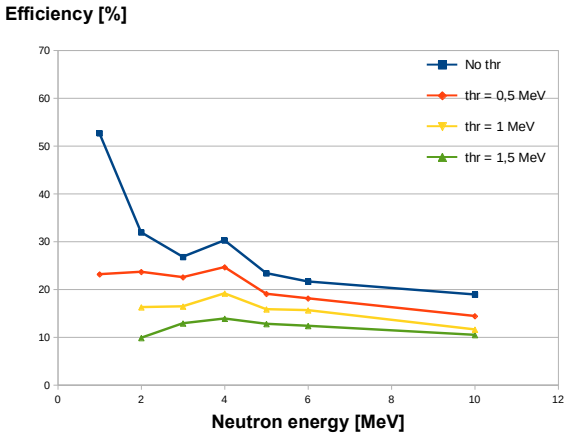

Figure 10. Corrected efficiency percentage values as a function of the neutron flux energy for the matrix configuration. The different curves are obtained for different elementary cell detection thresholds.

particles detected by each cell is obviously overestimated because of the cross-talk effects. Thus, the efficiency values, calculated with Equation 2, were corrected by the corresponding cross-talk probability values shown in Table 1.

The results, for the matrix configuration, are shown in Table 3 and plotted in Figure 10.

Higher efficiency values are observed for lower detection thresholds, as expected. Efficiency values bigger than 10% are found even with a detection threshold of 1 and 1.5 MeV for 10 MeV neutrons.

Similarly, the efficiency for the three-cluster configuration was evaluated simulating a flux of 10^6 neutrons impinging over the entire three-cluster configuration surface. Even in this case the efficiency values, calculated with Equation 2, were corrected by the corresponding cross-talk probability values shown in Table 1.

Table 4. Corrected efficiency percentage values evaluated for the three-cluster configuration for different neutron flux energy and different elementary cell detection thresholds.

Neutron Energy [MeV]	Efficiency [%] values corrected by CT for different thresholds [MeV]			
	0.0	0.5	1.0	1.5
1	73.36	47.52	-	-
2	72.39	55.62	39.57	23.90
3	67.08	58.29	43.54	34.68
4	70.68	61.33	47.43	35.26
5	62.90	53.49	44.01	36.04
6	59.72	51.72	45.05	35.64
10	54.04	43.62	35.39	31.94

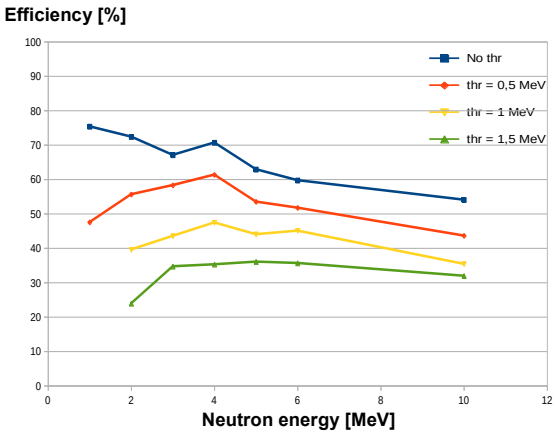

Figure 11. Corrected efficiency percentage values as a function of the neutron flux energy for the three-cluster configuration. The different curves are obtained for different elementary cell detection thresholds.

The results, for the three-cluster configuration, are shown in Table 4 and plotted in Figure 11.

From comparison of results in Figure 10 and Figure 11 it can be easily noticed that higher values of efficiency are obtained for the three-cluster configuration. Efficiency values bigger than 30 % are found even with a detection threshold of 1 and 1.5 MeV for 10 MeV neutrons.

5. Conclusion

In this paper two different geometrical configurations of the elementary detection cell of the NArCoS prototype were studied in terms of detection efficiency and cross-talk probability. Higher detection efficiency was found for the three-cluster configuration with respect to the matrix one. The cross-talk probability increases reasonably with the neutron energy and decreases at increasing of the detection thresholds. The evaluated cross-talk probability and efficiency values are very suitable for the NArCoS physics needs. This study demonstrates that EJ276-G is highly suitable to be the basic detection element of a neutron correlator for application in fundamental nuclear and applied physics. The study supports the project to construct the new correlator for neutron spectroscopy and reaction dynamics NArCoS. Other calculations will be done in the next future. All the calculation will keep into account the experimental needs and will be aimed at maximizing detection efficiency, energy resolution and position measurement accuracy and with the final goal of producing an efficient method for disentangling between true and a bad events (cross-talk events). In this scenario, the mechanical support and the use of an attenuator material between the cells in order to reduce the charged particles cross-talk probability will be simulated; different angular and energy neutron distributions, volume and edge effects, cosmic rays contributions to the background will be estimated.

Eventually, the final prototype of 64 elementary cells will be simulated and the efficiency and cross-talk probability will be evaluated. Calculations will be validated by experimental test performed with sources and in-beam experiments on different sub structures of

the final array. In this perspective, a single module prototype of the correlator made by 9 elementary adjacent cells is under construction, and an experiment, CROSS-TEST, was already approved at LNL and will be performed within the 2023. In this test the two geometrical configurations of the elementary cell here simulated will be experimentally studied.

Acknowledgements: *The whole project, involving the INFN (LNS, CT and MI units), University of Catania and the Politecnico of Milano, recently received financial support thanks to funding of Italian Government PRIN2021 ANCHISE (contract 2020H8YFRE). A prototype as demonstrator will be ready at the end of 2024.*

References

1. J. Van Driel et al., "Sequential ejectile decays and uncorrelated breakup processes in the ^{14}N+ ^{159}Tb reaction," *Physics Letters B*, **98**(5), 351–354, 1981. https://doi.org/10.1016/0370-2693(81)90923-0
2. A. Pagano et al., "Nuclear neck-density determination at Fermi energy with CHIMERA detector", *The European Physical Journal A*, **56**(102), 1–16, 2020. https://doi.org/10.1140/epja/s10050-020-00105-z
3. P. Russotto et al., "Production cross sections for intermediate mass fragments from dynamical and statistical decay of projectile-like fragments in ^{124}Sn +^{64}Ni and ^{112}Sn +^{58}Ni collisions at 35 A MeV", *Phys. Rev. C*, **91**(1), 014610, 2015. https://doi.org/10.1103/PhysRevC.91.014610
4. S. Pirrone et al., "Isospin influence on fragments production in ^{78}Kr + ^{40}Ca and ^{86}Kr + ^{48}Ca collisions at 10 MeV/nucleon", *Eur. Phys. J. A*, **55**(2), 22, 2019. https://doi:10.1140/epja/i2019-12695-4
5. P. Russotto et al., "Dynamical versus statistical production of intermediate mass fragments at Fermi energies", *Eur. Phys. J. A*, **56**(1), 12, 2020. https://doi:10.1140/epja/s10050-019-00011-z
6. G. Verde et al., "Probing transport theories via two proton source imaging", *Phys. Rev. C*, **67**(3), 034606, 2003. https://doi.org/10.1103/PhysRevC.67.034606
7. W. Bauer et al., "Hadronic interferometry in heavy ion collisions", *Ann. Rev. Nucl. Part. Sci.*, **42**, 77–100, 1992. https://doi.org/10.1146/annurev.ns.42.120192.000453
8. E. V. Pagano et al., "Statistical against dynamical PLF fission as seen by the IMF-IMF correlation functions and comparisons with CoMD model", *J. Phys. Conf. Ser.*, **1014**(1), 012011, 2018. https://doi.org/10.1088/17426596/1014/1/012011
9. N. Colonna et al., "A modular array for neutron spectroscopy in low-and intermediate-energy heavy-ion reactions", *Nucl. Instrum. Methods in Phys. Res. A*, **381**(2-3), 472–480, 1996. https://doi.org/10.1016/S0168-9002(96)00675-4
10. R. Ghetti et al., "Possibility to deduce the emission time sequence of neutrons and protons from the neutron-proton correlation function", *Phys. Rev. Lett.*, **87**, 102701, 2001. https://doi.org/10.1103/PhysRevLett.87.102701
11. E. Pagano et al., "The NArCoS project", *Il nuovo cimento C*, **41**(5), 1–7, 2018. https://doi.org/10.1393/ncc/i2018-18181-9
12. E. Pagano et al., "NArCoS project for nuclear physics and applications", *Il nuovo cimento C*43 (1) (2020) 1–9. https://doi.org/10.1393/ncc/i2020-20012-9
13. E. V. Pagano et al., "The NArCoS project: efficiency estimation and the cross talk problem studied through Monte Carlo simulations", *Journal of Physics: Conference Series*, **1643**(1), 012037, 2020. https://doi.org/10.1088/1742-6596/1643/1/012037
14. S. Nyibule, et al., "Birks scaling of the particle light output functions for the EJ299-33 plastic scintillator", *Nucl. Instrum. Methods in Phys. Res. A*, **768**, 141–145, 2014. https://doi.org/10.1016/j.nima.2014.09.056
15. E. Pagano et al., "Pulse shape discrimination of plastic scintillator EJ299-33 with radioactive sources", *Nucl. Instrum. Methods in Phys. Res. A*, **889**, 83–88, 2018. https://doi.org/10.1016/j.nima.2018.02.010
16. E. Pagano et al., "Measurements of pulse shape discrimination with EJ299-33 plastic scintillator using heavy ion reaction", *Nucl. Instrum. Methods in Phys. Res. A*, **905**, 47–52, 2018. https://doi.org/10.1016/j.nima.2018.07.034
17. M. Taggart et al., "Neutron-gamma discrimination via PSD plastic scintillator and SiPMs", *J. Phys.: Conf. Ser.*, **763**, 012007, 2016. https://doi.org/10.1088/1742-6596/763/1/012007
18. E. De Filippo, A. Pagano, "Experimental effects on dynamics and thermodynamics in nuclear reactions on the symmetry energy as seen by the CHIMERA 4π detector", *Eur. Phys. J. A*, **50**, 32, 2014. https://doi.org/10.1140/epja/i2014-14032-y
19. E. Pagano et al., "Status and perspective of FARCOS: A new correlator array for nuclear reaction studies", *EPJ Web of Conferences*, **117**, 10008, 2016. https://doi.org/10.1051/epjconf/201611710008
20. L. Acosta et al., "Campaign of measurements to probe the good performance of the new array FARCOS for spectroscopy and correlations", *J. Phys.: Conf. Ser.*, **730**, 012001, 2016. https://doi.org/10.1088/1742-6596/730/1/012001
21. D. Dell'Aquila et al., "Study of cluster structures in ^{10}Be and ^{16}C neutron-rich nuclei via break-up reactions", *EPJ Web of Conferences*, **117**, 06011, 2016. https://doi.org/10.1051/epjconf/201611706011
22. J. Bishop et al., "Experimental investigation of α condensation in light nuclei", *Phys. Rev. C*, **100**(3), 034320, 2019. https://doi.org/10.1103/PhysRevC.100.034320
23. N. Martorana et al., "First measurement of the isoscalar excitation above the neutron emission threshold of the pygmy dipole resonance in ^{68}Ni", *Phys. Lett. B*, **782**, 112–116, 2018. https://doi.org/10.1016/j.physletb.2018.05.019
24. N. Martorana, et al., "On the nature of the pygmy dipole resonance in ^{68}Ni", *Il nuovo cimento* C, **41**(5), 1–4, 2018. https://doi.org/10.1393/ncc/i2018-18199-y
25. P. Russotto, et al., "Status and perspectives of the INFN-LNS in-flight fragment separator", *J. Phys.: Conf. Ser.*, **1014**, 012016, 2018. https://doi.org/10.1088/1742-6596/1014/1/012016
26. N. Martorana, "Status of the FraISe facility and diagnostics system", *Il nuovo cimento C*, **44**(1), 1-10, 2021. https://doi.org/10.1393/ncc/i2021-21001-2
27. N. Martorana, L. Acosta, C. Altana, A. Amato, L. Calabretta, "The new fragment in-flight separator at INFN-LNS", *Il nuovo cimento C*, **45**(3), 1–7, 2022.

https://doi.org/10.1393/ncc/i2022-22063-2

28. T. Marchi et al., "The SPES facility at Legnaro National Laboratories", *J. Phys.: Conf. Ser.*, **1643**, 012036, 2020.
https://doi.org//10.1088/1742-6596/1643/1/012036
29. https://www.gsi.de/en/researchaccelerators/fair
30. Boretzky et al., "NeuLAND: The high-resolution neutron time-of-flight spectrometer for R3B at FAIR", *Nucl. Instrum. Methods in Phys. Res. A*, **1014**, 2021, 165701, 2021.
https://doi.org/10.1016/j.nima.2021.165701
31. S. Agostinelli, et al., "Geant4—a simulation toolkit", *Nucl. Instrum. Methods in Phys. Res. A*, **506**(3), 250–303, 2003.
https://doi.org/10.1016/S0168-9002(03)01368-8
32. J. Allison, et al, "Recent developments in Geant4", *Nucl. Instrum. Methods in Phys. Res. A*, **835**, 186–225, 2016.
https://doi.org/10.1016/j.nima.2016.06.125
33. E.V. Pagano, et al., "New frontend readout system for the NArCoS prototype", *LNS Activity report 2021-2022*, 144.